Correction of the Persistent Current Effect in Nb_3Sn Dipole Magnets

Vadim V. Kashikhin and Alexander V. Zlobin

***Abstract*—The paper describes a method and results of simulation of persistent current effect in high field Nb_3Sn dipole magnets being developed for the future hadron colliders. Simple and effective techniques of passive correction of the persistent current effect in superconducting accelerator magnets are proposed. Using of these techniques allows a significant reduction of sextupole and decapole field components induced by persistent currents in a coil.**

***Index Terms*—passive corrector, persistent currents, magnetization, superconducting magnet.**

I. Introduction

ACCELERATOR magnets must meet rather strong field quality requirements. Typically the low order field multipoles within 2/3 of magnet bore must be less than (1 to 2)$\cdot 10^{-4}$ of the main field component in operating field range. However, results of magnetic measurements in superconducting (SC) accelerator magnets show that the field quality deteriorates noticeably at low fields. This effect, known as the coil magnetization (or persistent current) effect, is caused by persistent currents in SC filaments. It is large at low fields but falls rapidly when the main field increases. The negative consequences of this effect are a decrease of magnet dynamic aperture and operating field range as well as an increase a complexity and cost of correcting systems. The situation is especially critical for high field accelerator magnets based on Nb_3Sn conductor. Commercially available Nb_3Sn strands provide a critical current density sufficient to achieve 11 to 13 T fields. However, the high critical current density and a large effective filament size produce a coil magnetization effect an order of magnitude larger than in NbTi magnets.

To correct this effect during machine operation a complicated field correcting system containing a variety of multipole correctors is used (active correction). Several methods of field quality correction based on superconducting and magnetic materials have also been proposed [1]-[4] (passive correction). Passive field correction would be very attractive in high field SC accelerator magnets if a reliable and inexpensive technique is developed. Results of calculations of the coil magnetization effect in Nb_3Sn accelerator magnets of different designs and the possibility of correction using a simple inexpensive technique based on thin iron strips are reported and discussed in this paper.

Manuscript received September 18, 2000.

This work was supported by the U.S. Department of Energy.

V. V. Kashikhin and A.V. Zlobin are with Fermi National Accelerator Laboratory, Fermilab, MS 316, P.O. Box 500, Batavia, IL 60510 (emails: vadim@fnal.gov, zlobin@fnal.gov).

II. Persistent Current Effect in High Field Nb_3Sn Dipole Magnets

Magnetic field in a magnet bore can be described in terms of normalized multipole coefficients according to the expression

$$B_y(x,y) + iB_x(x,y) = 10^{-4} \times B_1 \sum_{n=1}^{\infty} (b_n + ia_n) \left(\frac{x+iy}{R_{ref}} \right)^{n-1},$$

where $B_x(x,y)$ and $B_y(x,y)$ are horizontal and vertical field components, B_1 is the dipole component, R_{ref} = 1 cm is the reference radius; b_n and a_n are the normal and skew harmonic coefficients.

In high field SC magnets the field is mainly formed by the transport current in the coil and the iron yoke magnetization. Required field quality is achieved by an optimization of the coil and yoke geometry. Usually for accelerator magnets, geometrical harmonics with n<10 are eliminated. However, other magnetic design elements, such as coil, collar, beam pipe, etc., can also contribute to the field in the magnet aperture and need to be considered.

Finite element code OPERA 2D was used to simulate the coil magnetization effect in this study. It allows taking into account of a complicated geometry and real magnetic properties of all the magnetic elements. The coil magnetization was characterized by the magnetic properties of a Nb_3Sn strand with 1 mm diameter, critical current density of 1600 A/mm^2 at 12 T and 4.2 K and Cu/non-Cu ratio of 0.85, measured at the Fermilab short sample test facility [5]. Fig. 1 presents magnetization curves per strand volume for the first and consequent field cycles. The effective filament diameter derived from this curve is about 120 μm.

Accelerator magnets operate in a cycling mode. Therefore the magnetization curve for the second and subsequent cycles was used in our calculations. To assign the cable magnetic properties in the OPERA 2D model, the magnetization curve

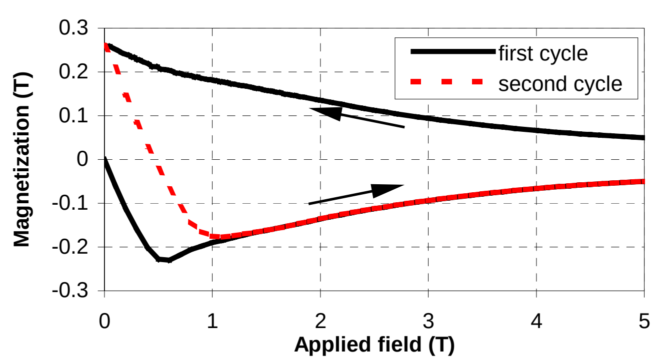

Fig.1. SC magnetization as a function of applied field for the first and subsequent magnetic cycles.

of SC strand was transformed into a B(H) curve according to the formula:

$$B(H) = \mu_0 H + M(\mu_0 H) \cdot \lambda_{str} \,,$$

where λ_{str} is the average packing factor of strands in the cable.

The coil magnetization effect was first computed for the shell-type (or cos-theta) and single-layer common coil magnets being developed at Fermilab for the Very Large Hadron Collider (VLHC) [6]-[7]. Fig. 2 (designs A and B) shows coil cross-sections of these magnets and the value of Cu/non-Cu ratio in strands. Since the coil magnetization contributes only a few tenths of percent to the total magnetic field, it would be difficult to distinguish this effect on a traditional field map plot (lines of equal total vector potential). For this reason Fig. 2 presents lines of vector potential produced by the coil magnetization only.

From Fig. 2 one can see that a cos-theta type magnet possesses a much stronger persistent current effect than a single-layer common coil design. This is quantitatively confirmed by the plots of relative sextupole and decapole components presented in Figs. 3-4. These plots show the addition of multipoles due to the coil magnetization effect only. Geometrical field errors and non-linear iron saturation effect were taken into account during simulation to obtain the correct field map but were subtracted from the presented dependencies. The plots indicate that the cos-theta magnet has a strong persistent current effect, resulting in a sextupole component deviation by -20 units at low field, while the common coil magnet has maximum sextupole deviations of –1.5 units (comparable to the yoke saturation effect). This observation might lead to the conclusion that block-type magnets are naturally preserved from the persistent current effect.

To check this assumption two other magnet designs with block-type coils were considered. As examples for numerical simulation, high field magnet designs being currently developed in other institutions [8]-[9] were used. Coil cross-section geometry of the magnets with flux lines produced by the coil magnetization are shown in Fig. 2 (designs C and D). One notices a significant magnetization flux through the coil bores. It follows from the plots in Figs. 3-4 that this flux results in multipole deviations comparable with those in the cos-theta magnet. The cause of the large persistent current effect in these magnets is likely to be the presence of field-forming auxiliary coils placed close to the aperture. Such coils do not have near boundary conditions at the bottom. This allows spreading of the magnetization flux in the horizontal direction on its way through the coil bore.

One can see that all the considered designs except the single-layer common coil magnet have a large persistent current effect. For present Nb_3Sn strands, the maximum value of b_3 at the bore field of 1 T is –20 to –30 units and the maximum value of b_5 is +3 to +9 units for different magnet designs. Since the superconductor magnetization is proportional to $J_c{\cdot}d_{eff}$, the effect even increases for the Nb_3Sn strands with higher J_c unless d_{eff} is significantly reduced. In order to decrease b_3 to a level below 10 units, d_{eff} must be reduced from 120 µm to less than 30 µm. One also notices that the effect rapidly decreases with increasing magnetic field. However, the sextupole is still larger than 10 units at B=2 T. Thus the problem cannot be solved by using a pre-injector based on iron-dominated magnets as it was suggested in [10]. One thus concludes that, in general, the coil magnetization effect in Nb_3Sn dipole magnets is large and requires correction.

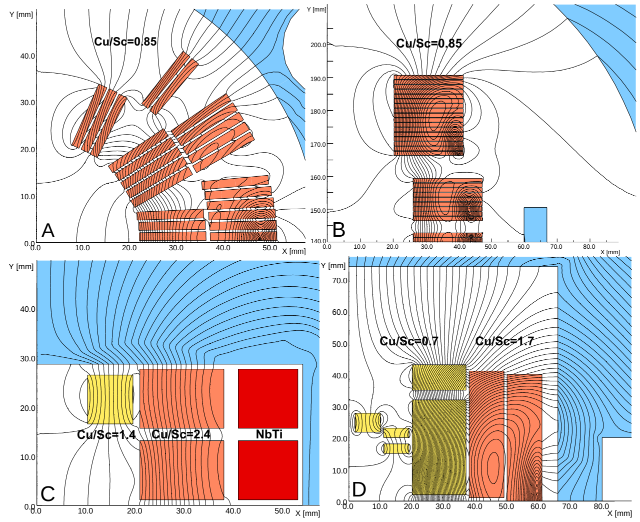

Fig. 2. Cross-sections of different magnets with flux lines produced by coil magnetization only (see the text). Flux increment between two adjacent lines is kept constant and equal $5\text{x}10^{-5}$ Wb/m in all field plots of this paper for easier illustrative comparison between different designs.

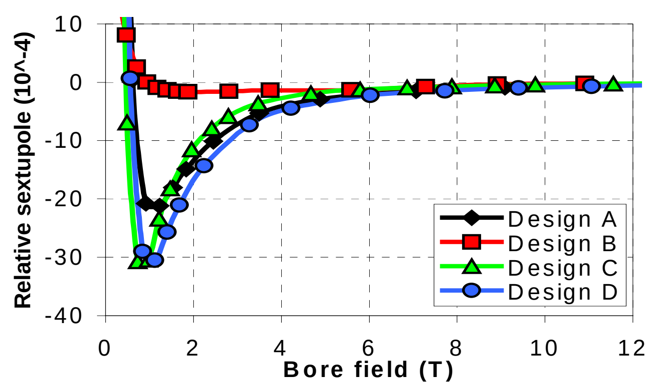

Fig. 3. Sextupole field component due to persistent currents in the coil.

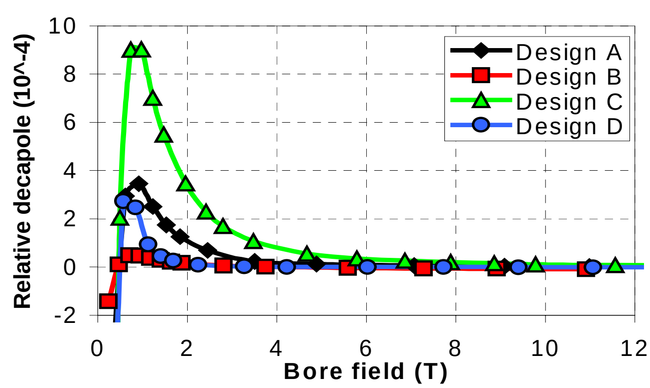

Fig. 4. Decapole field component due to persistent currents in the coil.

III. Correction of the Persistent Current Effect

A simple inexpensive method of passive correction of the persistent current effect in SC accelerator magnets based on iron strips is described below. Magnetic properties (magnetization and permeability) of the strip material used in this analysis are reported in Fig. 5. Simulation of passive correction was done for a Nb_3Sn cos-theta dipole magnet with a typical coil magnetization effect [6].

A. Thin iron strips inside the magnet aperture

In this approach the strips were installed on the outer surface of the beam pipe, and they work as the iron shims in conventional iron-dominated magnets. To find the optimal number, size and position of the correcting strips, preliminary calculations were performed with 0.2 mm thick and 2.58 mm wide strips placed with dipole symmetry on a cylindrical surface of 19.75 mm radius centered in the magnet bore. Fig. 6 shows the dependence of the low-order field multipole components generated by the strips as a function of their azimuthal position in the magnet bore at a field of 1 T. In this case all multipole components allowed by strip symmetry are present although high order harmonics are small. One can see that relatively small correcting strips produce large field multipoles, which can be used for correction of the coil magnetization effect.

Final geometry and position of the strips were optimized to simultaneously minimize sextupole and decapole deviations due to the coil magnetization effect. Initial position of the strips was established using Fig. 6. It was found that two 0.14 mm thick strips of 3.79 mm and 5.17 mm width, centered at azimuthal positions of 39 and 65 degrees from the coil midplane respectively are sufficient for simultaneous cancellation of sextupole and decapole field components [11]. The optimized position of the correcting strips and the magnetic flux distribution generated by the coil and strips magnetization are shown in Fig. 7 (left).

The correcting strips in this case do not noticeably reduce magnetization flux through the coil bore. However, since only the main (dipole) field component exists after correction no negative effect on the field quality is produced.

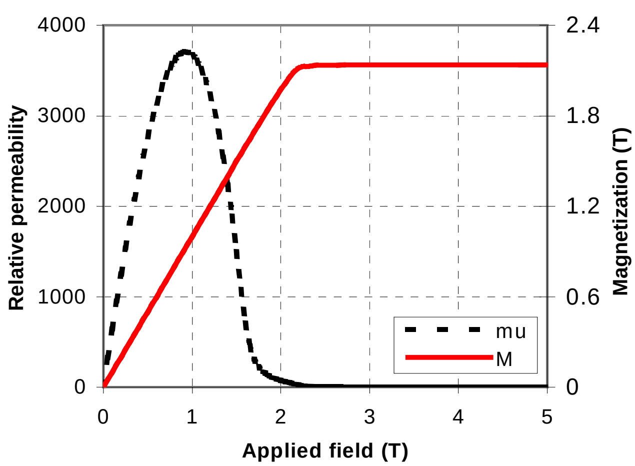

Fig. 5. Magnetization and relative permeability of the strip material.

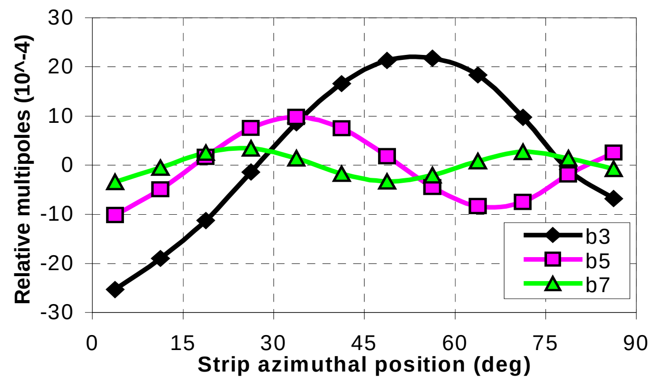

Fig. 6. Field multipoles as a function of the strip azimuthal position.

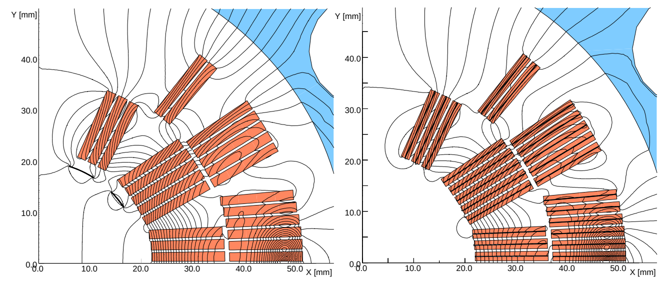

Fig. 7. Correction of coil magnetization effect by strips on the beam pipe (left) and strips inside of the cable (right).

B. Thin iron strips inside the coil

In this case, ferromagnetic strips were placed as a cable core. Such a method employs the idea of an internal compensation of the coil magnetization. Taking into account that SC materials possess a diamagnetic behavior in the relevant field region, it is possible to use ferromagnetic materials for compensation of SC magnetization. To estimate the amount of ferromagnetic material required for cancellation of the cable magnetization at some reference field H_{ref}, one can use the following expression

$$\lambda_{fe} = \lambda_{sc} \cdot \frac{M_{sc}(\mu_0 H_{ref})}{M_{fe}(\mu_0 H_{ref})} ,$$

where λ_{fe} and λ_{sc} are the packing factors of the iron strips and SC strands in the cable (coil), and M_{fe} and M_{sc} are the magnetization of the iron strips and SC strands respectively.

The formula above gives only a rough estimation of the required amount of ferromagnetic material in the coil. Due to field variation across the coil cross-section, different parts of the coil produce a magnetization effect of different strengths. This effect along with the non-linear properties of correcting strips can only be precisely analyzed using numerical techniques. If we assume a width of the iron core equal to the cable width, its thickness must be 57 µm to correct a sextupole component of size similar to that considered in the case with strips inside the aperture [12]. Fig. 7 (right) shows the coil cross-section with iron strips inside the cable and magnetization flux distribution in the magnet cross-section. One notices that the distribution of ferromagnetic material inside the coil reduces the coil magnetization effect by compensation of the total field produced by the SC magnetization.

C. Results and discussion

Calculated normalized sextupole and decapole field components before and after correction by two described above methods are shown in Figs. 8-9. These plots show that the relative sextupole component can be reduced by a factor of 5 at 1 T field by applying either of the correction techniques. By using correcting strips placed inside the aperture, the relative decapole component can be reduced by factor of 3.

Our data show that the proposed passive correction schemes increase the magnet dynamic range (ratio of operation and injection fields) from 4 to 12 (by factor of 3). In the second and subsequent cycles the correction is effective only at fields higher than 1 T for present Nb_3Sn strands. A further increase of magnet dynamic range toward lower field using these techniques is not possible because of the rapid increase of harmonics in this field region. The situation can only be improved by reducing the effective filament diameter in Nb_3Sn strands.

Sensitivity analysis of the magnetic field in the aperture to the strip geometry and misalignment is presented in [13]. The results show that tolerances on the strip thickness and width are 10% and their positioning must be within ±0.5 mm. All these numbers are acceptable from the practical viewpoint.

IV. Summary

The analysis of the field quality deviations due to the coil magnetization effect in Nb_3Sn high field dipoles of different designs shows that, for the presently achievable effective filament size of 100-120 microns in Nb_3Sn strands, the sextupole and decapole field components are rather large at low fields in most of the designs.

It was shown that simple techniques based on thin iron strips placed in the magnet bore or inside the coil in the form of a cable core or inter-turn spacers, provide an effective correction (compensation) of the coil magnetization effect. By using the proposed techniques the injection field in magnets can be reduced to 1 T, significantly increasing magnet dynamic range. Further reduction of the injection field in Nb_3Sn accelerator magnets can then be achieved by decreasing the effective filament size. In this case requirements on minimal effective filament size in Nb_3Sn strands will be driven by conductor stability and cost considerations.

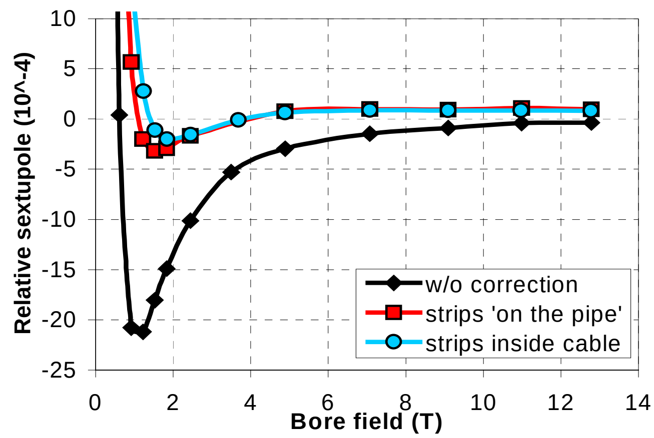

Fig. 8. Sextupole component with and without correction.

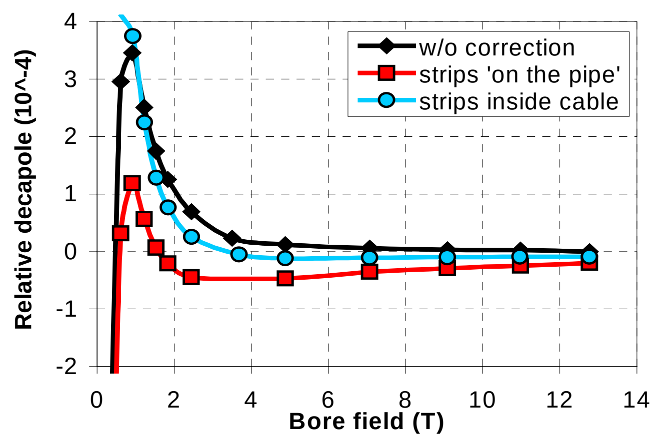

Fig. 9. Decapole component with and without correction.

References

[1] B. C. Brown, H.E. Fisk and R. Hanft, "Persistent current fields in Fermilab Tevatron magnets", IEEE Transactions on Magnetics, MAG-21, No. 2, 1985, p.979.

[2] M. A. Green, "Control of the fields due to superconductor magnetization in the SSC magnets", IEEE Transaction on Magnetics, MAG-23, No.2, 1987, p.506.

[3] M. A. Green, "Passive superconductor a viable method of controlling magnetization multipoles in the SSC dipole", IISSC Supercollider 1, Plenum Press, NY, 1989, p.351.

[4] E. W. Collings et al., "Design of multifilamentary strands for SSC dipole magnets", IISSC Supercollider 2, Plenum Press, NY, 1990, p.581.

[5] C. Boffo, "Magnetization measurements at 4.2 K of multifilamentary superconducting strands", thesis of University of Udine (Italy), December 1999.

[6] G. Ambrosio et al., "Magnetic design of the Fermilab 11 T Nb_3Sn short dipole model", IEEE Transactions on Applied Superconductivity, v. 10, No. 1, March 2000, p.322.

[7] V.V. Kashikhin, A.V. Zlobin, "Magnetic designs of 2-in-1 Nb_3Sn dipole magnets for VLHC", IEEE Transactions on Applied Superconductivity, ASC2000, submitted for publication.

[8] C. Battle et al., "Optimization of block-coil dipoles for hadron colliders", Proceedings of the 1999 Particle Accelerator Conference, NY, 1999, p.2936.

[9] R. Gupta, "BNL phase II common coil magnet program", VLHC Magnet Technologies Workshop, Fermilab, May 24-26 2000, published on the web: http://www.vlhc.org.

[10] R. Gupta, S. Ramberger, "Field quality optimization in a common coil magnet design", IEEE Transactions on Applied Superconductivity, v. 10, No. 1, March 2000, p.326.

[11] V.V. Kashikhin, A.V. Zlobin, "Correction of coil magnetization effect in Nb_3Sn high field dipole magnet using thin iron strips", Fermilab internal note*, TD-99-048, October 15, 1999.

[12] V.V. Kashikhin, A.V. Zlobin, "Compensation of strand magnetization in superconducting rutherford cables by thin iron core", Fermilab internal note*, TD-00-011, February 4, 2000.

[13] V.V. Kashikhin, A.V. Zlobin, "Sensitivity of Field Harmonics in Nb_3Sn Dipole Magnet to the Correction Strip Position", Fermilab internal note*, TD-99-068, December 7, 1999.

* Accessible from the web: http://tdserver1.fnal.gov/tdlibry/TD-Notes/.